Modeling of Hysteresis Losses in Ferromagnetic Laminations under Mechanical Stress

P. Rasilo[1], D. Singh[1], U. Aydin[1], F. Martin[1], R. Kouhia[2], A. Belahcen[1], A. Arkkio[1]

[1]Department of Electrical Engineering and Automation, Aalto University, Espoo, Finland
[2]Department of Mechanical Engineering and Industrial Systems, Tampere University of Technology, Tampere, Finland

A novel approach for predicting magnetic hysteresis loops and losses in ferromagnetic laminations under mechanical stress is presented. The model is based on combining a Helmholtz free energy -based anhysteretic magnetoelastic constitutive law to a vector Jiles-Atherton hysteresis model. This paper focuses only on unidirectional and parallel magnetic fields and stresses, albeit the model is developed in full 3-D configuration in order to account also for strains perpendicular to the loading direction. The model parameters are fitted to magnetization curve measurements under compressive and tensile stresses. Both the hysteresis loops and losses are modeled accurately for stresses ranging from –50 to 80 MPa.

Index Terms—Helmholtz free energy, magnetic hysteresis, magnetoelasticity, magnetostriction, strain, stress.

I. INTRODUCTION

DEPENDENCY of iron losses on mechanical stresses and strains remains a problem in accurate design and analysis of electrical machines. The increase of power losses due to mechanical processing of the core laminations [1] is generally associated to the plastic deformations and residual stresses caused by the process. In addition, temperature gradients and centrifugal forces give rise to additional mechanical loadings in the cores.

Different approaches for both theoretical [2]-[3] and experimental [4]-[5] formulations for coupled multiaxial magnetomechanical field problems have been studied quite recently. However, modeling of the losses has received less attention, and the presented loss models have typically been based on large amounts of experimental data. For example in [1] and [5], measured iron-loss and magnetization curves were used in finite-element (FE) analysis to study the effects of shrink-fitting and punching in electrical machine stator cores. After the developments of [6], theoretical models for hysteresis effects under mechanical loadings have not received very much attention. Especially multiaxial modeling approaches for hysteresis losses have been starting to gain ground only during the recent years [7], [8].

In [7], an interesting approach was taken for coupling the single-valued (SV) constitutive law of [3] to the vector Jiles-Atherton (JA) hysteresis model. In this paper, we implement a similar extension for the energy-based SV constitutive law of [2]. The SV constitutive law is first derived by partial differentiation of a Helmholtz free energy density function expressed using the magnetic flux density vector and total

strain tensor. This SV model is then used in the JA model to replace the function for the anhysteretic magnetization. In addition, the loss parameter k of the original JA model is replaced by a tensor function of the total stress. After the model parameters are fitted to unidirectional magnetization curves measured under different stresses, the model predicts the hysteresis losses accurately over a stress range of –50 to 80 MPa. The model also accounts for the decreasing permeability and increasing losses under high tensile stress.

II. MODELS

A. Single-Valued Constitutive Law

The 3-D single-valued material model is developed similarly to [2] and [9]. The flux density vector B (of size 3×1) and the total strain tensor ε (3×3) are chosen as the independent state variables. The magnetization M and magnetostrictive stress σ_{me} are expressed as partial derivatives of a Helmholtz free energy density ψ with respect to B and ε:

$$M(B,\varepsilon) = -\left(\frac{\partial \psi(B,\varepsilon)}{\partial B}\right)^{\mathrm{T}} \qquad (1)$$

$$\sigma_{me}(B,\varepsilon) = \frac{\partial \psi(B,\varepsilon)}{\partial \varepsilon}. \qquad (2)$$

The magnetic field strength is $H = v_0 B - M$, and the total stress $\sigma = \sigma_{me} + \sigma_{mag}$ also includes the purely electromagnetic contribution from the Maxwell stress tensor

$$\sigma_{mag} = v_0\left(BB^{\mathrm{T}} - \frac{1}{2}(B \cdot B)I\right) + (M \cdot B)I - BM^{\mathrm{T}}, \qquad (3)$$

in which $v_0 = 1/\mu_0$ is the reluctivity of free space and I is the 3×3 unit tensor.

The integrity basis of an isotropic scalar function ψ depending on one vector B and one tensor ε includes six scalar invariants, which in this case are written as

$$I_1 = \operatorname{tr} \boldsymbol{\varepsilon}, \quad I_2 = \frac{1}{2} \operatorname{tr} \boldsymbol{\varepsilon}^2, \quad I_3 = \det \boldsymbol{\varepsilon},$$

$$I_4 = \frac{\boldsymbol{B} \cdot \boldsymbol{B}}{B_{\mathrm{ref}}^2}, \quad I_5 = \frac{\boldsymbol{B} \cdot (\tilde{\boldsymbol{\varepsilon}} \boldsymbol{B})}{B_{\mathrm{ref}}^2}, \quad I_6 = \frac{\boldsymbol{B} \cdot (\tilde{\boldsymbol{\varepsilon}}^2 \boldsymbol{B})}{B_{\mathrm{ref}}^2}, \tag{4}$$

where $B_{\mathrm{ref}} = 1$ T. Invariants I_1-I_3 describe purely elastic behavior, and I_3 is not used here since linear elasticity is assumed. I_4 describes purely magnetic behavior. I_5 and I_6 describe the magnetoelastic coupling, and are written using the deviatoric strain

$$\tilde{\boldsymbol{\varepsilon}} = \boldsymbol{\varepsilon} - \frac{1}{3} (\operatorname{tr} \boldsymbol{\varepsilon}) \boldsymbol{I} \tag{5}$$

in order to eliminate the effect of hydrostatic pressure on the magnetization properties [10].

The problem of forming a coupled magnetomechanical constitutive law has now been reduced to finding a suitable expression for the Helmholtz energy density (in J/m^3) in the form $\psi(I_1, I_2, I_4, I_5, I_6)$. Here we have chosen the expression

$$\psi = \frac{1}{2} \lambda I_1^2 + 2\mu I_2 + \sum_{i=0}^{n_\alpha-1} \frac{g_i(I_1)}{i+1} I_4^{i+1} + \sum_{i=0}^{n_\beta-1} \beta_i I_5^{i+1} + \sum_{i=0}^{n_\gamma-1} \gamma_i I_6^{i+1}, \tag{6}$$

in which the functions

$$g_i(I_1) = \alpha_i \exp\left(\frac{4(i+1)}{3} I_1 \right) - \begin{cases} \dfrac{v_0}{8}, & \text{if } i = 0 \\ 0, & \text{if } i > 0 \end{cases} \tag{7}$$

have been derived so as to obtain isochoric magnetostriction under purely magnetic loading [9]. λ and μ are the Lamé constants of the material, and α_i, β_i and γ_i are parameters determined by fitting. The first two terms in (6) yield Hooke's law and account for the purely mechanical behavior, while the last three terms account for the magnetomechanical coupling. The summation term in the middle (with $n_\alpha > 1$) accounts for the nonlinear $M(B, \boldsymbol{\varepsilon})$ relationship. Finally, the quadratic dependence of invariant I_6 on $\boldsymbol{\varepsilon}$ allows modeling the decreasing permeability under both compressive and high tensile stresses.

B. Jiles-Atherton Model

The hysteretic magnetization behavior is modeled following the inverse vector JA hysteresis model described in [11]. The model is summarized with the following five equations:

$$\boldsymbol{H}_{\mathrm{eff}} = \boldsymbol{H} + \alpha \boldsymbol{M}, \tag{8}$$

$$\boldsymbol{M}_{\mathrm{an}} = f\left(|\boldsymbol{H}_{\mathrm{eff}}|\right) \frac{\boldsymbol{H}_{\mathrm{eff}}}{|\boldsymbol{H}_{\mathrm{eff}}|}, \tag{9}$$

$$\boldsymbol{d} = \boldsymbol{M}_{\mathrm{an}} - \boldsymbol{M}_{\mathrm{irr}} \text{ and } \delta = \frac{d\boldsymbol{B}}{dt} \cdot \boldsymbol{d}, \tag{10}$$

$$\frac{d\boldsymbol{M}_{\mathrm{irr}}}{d\boldsymbol{H}_{\mathrm{eff}}} = \begin{cases} k^{-1} \dfrac{\boldsymbol{d}\boldsymbol{d}^{\mathrm{T}}}{|\boldsymbol{d}|}, & \text{if } |\boldsymbol{d}| > 0 \text{ and } \delta > 0 \\ \boldsymbol{0}, & \text{otherwise}, \end{cases} \tag{11}$$

$$\frac{d\boldsymbol{M}}{d\boldsymbol{H}_{\mathrm{eff}}} = c \frac{d\boldsymbol{M}_{\mathrm{an}}}{d\boldsymbol{H}_{\mathrm{eff}}} + (1-c) \frac{d\boldsymbol{M}_{\mathrm{irr}}}{d\boldsymbol{H}_{\mathrm{eff}}}. \tag{12}$$

Here $\boldsymbol{H}_{\mathrm{eff}}$ is the effective field strength experienced by the domains, and $\boldsymbol{M}_{\mathrm{an}}$ and $\boldsymbol{M}_{\mathrm{irr}}$ are the anhysteretic and irreversible components of the total magnetization. f is typically a sigmoid-shaped scalar function representing the anhysteretic magnetization, and α, k and c are fitting parameters. Parameter k describes the magnitude of domain-wall pinning and is the most influential parameter considering the coercive field strength and the hysteresis losses.

The magnetomechanical coupling is introduced in the JA model by replacing (9) by the SV model (1). Since the JA model requires obtaining $\boldsymbol{M}_{\mathrm{an}}$ as a function of $\boldsymbol{H}_{\mathrm{eff}}$, but the input of the SV model is $\boldsymbol{B}$, we iterate the anhysteretic magnetization for a given $\boldsymbol{H}_{\mathrm{eff}}$ from (1) using the Newton-Raphson (NR) method. We are searching for an equivalent flux density $\boldsymbol{B}_{\mathrm{an}} = \mu_0(\boldsymbol{H}_{\mathrm{eff}} + \boldsymbol{M}_{\mathrm{an}})$, which for a given stress $\boldsymbol{\varepsilon}$ satisfies $\boldsymbol{M}(\boldsymbol{B}_{\mathrm{an}}, \boldsymbol{\varepsilon}) = \boldsymbol{M}_{\mathrm{an}}$. We thus write a residual vector and a Jacobian matrix, respectively, as

$$\boldsymbol{r}(\boldsymbol{B}_{\mathrm{an}}) = \boldsymbol{M}(\boldsymbol{B}_{\mathrm{an}}, \boldsymbol{\varepsilon}) - (v_0 \boldsymbol{B}_{\mathrm{an}} - \boldsymbol{H}_{\mathrm{eff}}) \tag{13}$$

$$\boldsymbol{J}(\boldsymbol{B}_{\mathrm{an}}) = \frac{d\boldsymbol{r}(\boldsymbol{B}_{\mathrm{an}})}{d\boldsymbol{B}_{\mathrm{an}}} = \frac{\partial \boldsymbol{M}(\boldsymbol{B}_{\mathrm{an}}, \boldsymbol{\varepsilon})}{\partial \boldsymbol{B}_{\mathrm{an}}} - v_0 \boldsymbol{I}. \tag{14}$$

C. Stress-Dependent Coercive Field

The effect of stress on the coercive field strength is modeled by introducing stress-induced anisotropy to the JA model pinning parameter k in (11). The scalar k is replaced by a second-order tensor $\boldsymbol{k}$ (3×3), which is an isotropic function of the total stress $\boldsymbol{\sigma}$, meaning that

$$\boldsymbol{k}(\boldsymbol{R}\boldsymbol{\sigma}\boldsymbol{R}^{\mathrm{T}}) = \boldsymbol{R}\boldsymbol{k}(\boldsymbol{\sigma})\boldsymbol{R}^{\mathrm{T}}, \tag{15}$$

for any coordinate transformation matrix $\boldsymbol{R}$. The tensorial integrity basis of such an isotropic function is $\{\boldsymbol{I}, \boldsymbol{\sigma}, \boldsymbol{\sigma}^2\}$, which means that $\boldsymbol{k}$ can be formed as a linear combination

$$\boldsymbol{k}(\boldsymbol{\sigma}) = k_0 \left(\boldsymbol{I} + a\boldsymbol{\sigma} + b\boldsymbol{\sigma}^2 \right), \tag{16}$$

in which k_0, a and b depend only on the scalar invariants of $\boldsymbol{\sigma}$. As a first approximation, we assume that k_0, a and b are constant, and they are treated as fitting parameters. The tensor $\boldsymbol{k}$ obtained from (16) is coaxial with $\boldsymbol{\sigma}$, meaning that both tensors have the same principal axes.

III. MEASUREMENT SETUP

A custom-built setup was used to measure magnetization properties of electrical steel sheet samples under uniaxial

stress. A picture of the setup is shown in Fig. 1. A rectangular sample is stressed using a manual screw, and a spring is connected in series with the sample in order to allow accurate control of the force.

The sample is magnetized using two vertical cores. The average flux density is measured using a coil wound around the sample, and the surface field strength is measured using an *H*-coil. The signals are recorded using a National Instruments USB-6251 BNC data acquisition system. The average flux density is controlled to be sinusoidal by a feedback control system implemented using the Data Acquisition Toolbox of MATLAB. The control is implemented similarly to [12] and iteratively searches for an input voltage waveform which yields a sinusoidal flux density in the sample.

IV. RESULTS

The parameters α_i, β_i and γ_i of the SV model were first fitted by least-squares comparison to magnetization curve measurements for a 0.5-mm nonoriented Fe-Si sheet sample. The number of terms in the polynomials of (6) were $n_\alpha = 7$, $n_\beta = 1$, $n_\gamma = 2$. The magnetization loops were measured at 1.7 T sinusoidal flux densities under nine different stresses $\boldsymbol{\sigma}_\mathrm{L}$ ranging from 50 MPa compression (–) to 80 MPa tension (+). Fig. 2 shows the results of fitting the parameters to the *H*-averaged magnetization loops at four different stress values. The parameter values are given in Table I. For a given load $\boldsymbol{\sigma}_\mathrm{L}$ and flux density $\boldsymbol{B}$, the total strain $\boldsymbol{\varepsilon}$ has been iterated with the NR method by expressing the tensors using the Voigt notation, and writing the residual and Jacobian matrix as:

$$\boldsymbol{r}(\boldsymbol{\varepsilon}) = \boldsymbol{\sigma}(\boldsymbol{B}, \boldsymbol{\varepsilon}) - \boldsymbol{\sigma}_\mathrm{L} \tag{17}$$

$$\boldsymbol{J}(\boldsymbol{\varepsilon}) = \frac{d\boldsymbol{r}(\boldsymbol{\varepsilon})}{d\boldsymbol{\varepsilon}} = \frac{\partial \boldsymbol{\sigma}(\boldsymbol{B}, \boldsymbol{\varepsilon})}{\partial \boldsymbol{\varepsilon}}. \tag{18}$$

It is emphasized that despite the unidirectional flux density and stress, using the multiaxial model is essential since the perpendicular components of $\boldsymbol{\varepsilon}$ also become nonzero. The model fits reasonably well and is able to predict the quadratic dependency of the magnetization curves on the stress, so that both compression and high tension reduce the permeability from the zero-stress case. This effect is not observed with the energy definitions of [3] and [7], although the effect can be taken into account with an additional correction term [8].

We next fitted the pinning parameters k_0, a, b, as well as α and c of the JA model. The fitting was done by comparing both the simulated ascending major-loop branch and the hysteresis losses to the measured ones in the least-squares sense. Fig. 3 shows the results of the fitting at the same four stresses as in the SV case. The parameter values are given in Table I. Both the loop shapes and the coercive fields are reasonably modeled. Finally, a good correspondence is observed in Fig. 4 between the measured and modeled hysteresis losses also at the other five stress values used in the measurements. The errors between the measured and simulated field strengths vary between 3.2 % and 7.8 %.
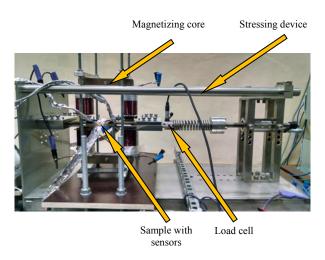

Fig. 1. Experimental setup for measuring unidirectional magnetization curves under stresses parallel to the magnetic field.
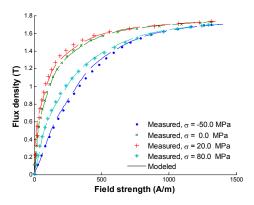

Fig. 2. Fitting the parameters α_i, β_i and γ_i of the single-valued model to *H*-averaged *B-H* curve measurements at different compressive and tensile stresses.
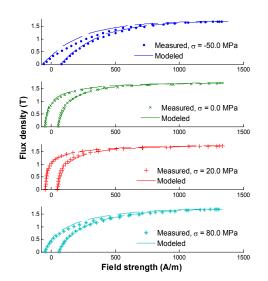

Fig. 3. Fitting the hysteresis model parameters k_0, a, b, α and c to the *B-H* curve measurements at different compressive and tensile stresses
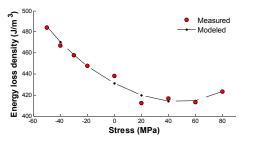
Fig. 4. Comparison of modeled and measured static hysteresis losses at different compressive and tensile stresses.

TABLE I
USED AND FITTED PARAMETER VALUES

Parameter	Value	Parameter	Value
λ	145.1 GPa	β_0	$-17.5 \times 10^{-3}\ v_0\ T^2$
μ	68.3 GPa	γ_0	$988\ v_0\ T^2$
α_0	$-0.499\ v_0\ T^2$	γ_1	$1.40 \times 10^9\ v_0\ T^2$
α_1	$-0.229 \times 10^{-3}\ v_0\ T^2$	k_0	76.6 A/m
α_2	$0.838 \times 10^{-3}\ v_0\ T^2$	a	-1.49 GPa^{-1}
α_3	$-1.12 \times 10^{-3}\ v_0\ T^2$	b	12.7 GPa^{-2}
α_4	$0.725 \times 10^{-3}\ v_0\ T^2$	α	7.27×10^{-5}
α_5	$-0.224 \times 10^{-3}\ v_0\ T^2$	c	0.155
α_6	$0.0268 \times 10^{-3}\ v_0\ T^2$		

V. DISCUSSION AND CONCLUSION

A hysteretic magnetomechanical constitutive law was presented and fitted to magnetization curve measurements under unidirectional magnetic field and parallel stress. The results show that the model is suitable for predicting magnetization curves and hysteresis losses in mechanically loaded laminations.

The accuracy of the SV model can rather easily be improved by increasing n_α, n_β and n_γ in (6), which also increases the number of the fitting parameters. One difficulty in the model is that (1) and (6) result in a polynomial expression of M as a function of B. Since the $M(B)$ relationship is rather linear at low fields and quickly saturates at higher fields, a polynomial is not very suitable for this purpose. Thus care has to be taken to ensure that the model does not result in S-shaped $B(H)$ curves with negative differential permeabilities. Better results can perhaps be obtained by writing the polynomial expression for the $H(B)$ relationship instead of $M(B)$, which requires slight modifications in (6) and (7).

The $v_0/8$ term in (7) is needed for obtaining isochoric magnetostriction under purely magnetic loading. However, inclusion of this term worsens the parameter fitting and can result in negative differential permeabilities, especially at low tensile stresses when the $B(H)$ curves are steeper. This term was thus omitted from the model in this paper. This causes some error in the volume magnetostriction, but ensures a positive differential permeability also under multiaxial stress [13] and keeps the NR iteration (13)-(14) stable.

The need for iterating the $M_{an}(H_{eff})$ relationship using (13)-(14) is a drawback if the model is to be implemented in numerical calculations tools, for example in FE solvers. Although the NR method typically converges in 2-3 iterations, this significantly increases the computation time compared to an explicit material model. The iteration could be avoided by developing the SV model using the field strength H as the variable instead of the flux density B. On the other hand, if hysteresis does not need to be considered during the solution, the B-based model is more comfortable with magnetic vector potential formulations. Since the mechanical state variable is the total strain, the model is directly suitable for solving displacement fields.

REFERENCES

[1] K. Fujisaki, R. Hirayama, T. Kawachi, S. Satou, C. Kaidou, M. Yabumoto, T. Kubota, "Motor Core Iron Loss Analysis Evaluating Shrink Fitting and Stamping by Finite-Element Method," *IEEE Trans. Magn.*, Vol. 43, No. 5, pp. 1950-1954, May 2007.

[2] K. Fonteyn, A. Belahcen, R. Kouhia, P. Rasilo, A. Arkkio, "FEM for Directly Coupled Magneto-Mechanical, Phenomena in Electrical Machines," *IEEE Trans. Magn.*, Vol. 46, No. 8, pp. 2923-2926, August 2010.

[3] L. Bernard, X. Mininger, L. Daniel, G. Krebs, F. Bouillaut, M. Gabsi, "Effect of Stress on Switched Reluctance Motors: A Magneto-Elastic Finite-Element Approach Based on Multiscale Constitutive Laws," *IEEE Trans. Magn.*, Vol. 47, No. 9, pp. 2171-2178, September 2011.

[4] H. Ebrahimi, Y. Gao, H. Dozono, K. Muramatsu, "Coupled Magneto-Mechanical Analysis in Isotropic Materials Under Multiaxial Stress," *IEEE Trans. Magn.*, Vol. 50, No. 2, February 2014.

[5] D. Miyagi, N. Maeda, Y. Ozeki, K. Miki, N. Takahashi, "Estimation of Iron Loss in Motor Core With Shrink Fitting Using FEM Analysis," *IEEE Trans. Magn.,* Vol. 45, No. 3, pp. 1704-1707, March 2009.

[6] M. J. Sablik, D. C. Jiles, "Coupled Magnetoelastic Theory of Magnetic and Magnetostrictive Hysteresis," *IEEE Trans. Magn.*, Vol. 29, No. 3, pp. 2113-2123, July 1993.

[7] L Bernard, L. Daniel, "Effect of stress on magnetic hysteresis losses in a switched reluctance motor: application to stator and rotor shrink-fitting," *IEEE Trans. Magn.* (in press).

[8] L. Daniel, M. Rekik, O. Hubert, "A multiscale model for magneto-elastic behaviour including hysteresis effects," *Arch. Appl. Mech.*, Vol. 84, pp. 1307-1323, 2014.

[9] K. Fonteyn, "Energy-Based Magneto-Mechanical Model for Electrical Steel Sheets," Ph.D. dissertation, Aalto University, 2010. Available at: http://lib.tkk.fi/Diss/2010/isbn9789526032887/.

[10] L. Daniel, "An Analytical Model for the Effect of Multiaxial Stress on the Magnetic Susceptibility of Ferromagnetic Materials," *IEEE Trans. Magn.*, Vol. 49, No. 5, pp. 2037-2040, May 2013.

[11] J. Gyselinck, P. Dular, N. Sadowski, J. Leite, J. P. A. Bastos, "Incorporation of a Jiles-Atherton vector hysteresis model in 2D FE magnetic field computations," *COMPEL*, Vol. 23, No. 3, pp. 685-693, 2004.

[12] K. Matsubara, N. Takahashi, K. Fujiwara, T. Nakata, M. Nakano, H. Aoki, "Acceleration Technique of Waveform Comtrol for Single Sheet Tester," *IEEE Trans. Magn.*, Vol. 31, No. 6, pp. 3400-3402, November 1995.

[13] U. Aydin, P. Rasilo, D. Singh, A. Lehikoinen, A. Belahcen, A. Arkkio, "Coupled Magneto-Mechanical Analysis of Iron Sheets Under Biaxial Stress," *IEEE Trans. Magn.* (under review).